

Unveiling of Bragg glass to vortex glass transition by an ac driving force in a single crystal of $\text{Yb}_3\text{Rh}_4\text{Sn}_{13}$

Santosh Kumar,^{1,*} Ravi P. Singh,^{2,†} A. Thamizhavel,² C. V. Tomy,¹ and A. K. Grover^{2,3,‡}

¹*Department of Physics, Indian Institute of Technology Bombay, Mumbai 400076, India.*

²*Department of Condensed Matter Physics and Materials Science,
Tata Institute of Fundamental Research, Mumbai 400005, India.*

³*Department of Physics, Panjab University, Chandigarh 160014, India.*

Abstract

We present here some striking discrepancies in the results of ac and dc magnetization measurements performed in a single crystal of low T_c superconductor, $\text{Yb}_3\text{Rh}_4\text{Sn}_{13}$. Fingerprint of a transition from an ordered vortex lattice *à la* Bragg glass (BG) phase to a partially-disordered vortex glass (VG) like phase gets unearthed under the influence of an ac driving force present inevitably in the isothermal ac susceptibility ($\chi'(H)$) measurements. In contrast to its well-known effect of improving the state of spatial order in the vortex matter, the ac drive is surprisingly found to promote disorder by assisting the BG to VG transition to occur at a lower field value in this compound. On the other hand, the isothermal dc magnetization ($M-H$) scans, devoid of such a driving force, do not reveal this transition; they instead yield signature of another order-disorder transition at elevated fields, viz., peak effect (PE), located substantially above the BG to VG transition observed in $\chi'(H)$ runs. Further, the evolution of PE feature with increasing field as observed in isofield ac susceptibility ($\chi'(T)$) plots indicates emergence of an ordered vortex configuration (BG) from a disordered phase above a certain field, H^* (~ 4 kOe). Below H^* , the vortex matter created via field-cooling (FC) is found to be better spatially ordered than that prepared in zero field-cooled (ZFC) mode. This is contrary to the usual behavior anticipated near the high-field order-disorder transition (PE) wherein a FC state is supposed to be a supercooled disordered phase and the ZFC state is comparatively better ordered.

PACS numbers: 74.25.Op, 74.25.Ha, 74.25.Dw

Keywords: Peak effect, second magnetization peak, generic vortex phase diagram.

I. INTRODUCTION

In the context of the mixed state of a type-II superconductor, the seminal discovery [1, 2] of a well-ordered thermodynamic phase, viz., Bragg glass (BG) exhibiting Bragg's reflections, and its possible transition(s) [3] to a disordered phase devoid of Bragg's reflections had lead to a generic vortex phase diagram [4] applicable to almost all pinned superconductors. Owing to the possibility of a sudden proliferation of dislocations on progressively increasing the magnetic field at a constant temperature, the quasi-long range ordered BG phase is anticipated [1, 2] to transform first into a multi-domain (partially disordered) vortex glass (VG) phase. Such a transition usually reflects as a second peak in (isothermal) magnetization ($M-H$) loops, termed as the second magnetization peak (SMP) anomaly [5–11]. Thereafter, at elevated fields closer to the upper critical field ($H_{c2}(T)$), there occurs another anomaly, known as the quintessential peak effect (PE) phenomenon [3, 9, 10, 12–18] in field/temperature variation in critical current density, $j_c(H, T)$. The PE is argued [12] to signal the collapse of the elasticity of an ordered vortex lattice at a rate faster than the pinning force density near $H_{c2}(T)$.

Although theoretical treatment related to the BG to

VG transition exists in the literature (for example, as in Ref. [2]), however, the experimental tools, particularly those employed to explore the bulk pinning properties, such as, the dc magnetization ($M-H$) measurements do not always capture this transition. Therefore, in the context of vortex phase diagram studies, it is tempting to ask a question- *Is the BG to VG phase transition generic?* If it is so, then this anomaly must get exposed in the $H-T$ space of all pinned superconductors, possessing a certain amount of quenched disorder. To address this issue, we have investigated via detailed magnetization measurements, a low T_c superconductor $\text{Yb}_3\text{Rh}_4\text{Sn}_{13}$, which has so far been reported [14–16] to display only the PE phenomenon. A claim of the presence of SMP anomaly (or its counterpart) in this compound has so far not been made by anyone. We have now found that the BG to VG (akin to SMP anomaly) transition in this compound gets exposed prior to the onset of PE under the influence of an ac driving force present in the (isothermal) ac susceptibility scans ($\chi'(H)$). Counter-intuitively, shaking of the vortex array by an ac drive in the present study has been seen to promote the spatial disordering in the vortex matter by assisting the BG to VG transition process. This observation is in complete contrast to the usual role of an ac driving force, which is to improve the state of spatial order in multi-domain vortex matter as reflected [17] by the enhanced brightness of the Bragg spots in the field-temperature phase space prior to crossover to the PE region in the vortex phase diagram. Another interesting aspect of the present study is a revelation of the inequality $j_c^{FC}(H) < j_c^{ZFC}(H)$ at lower fields (below a characteristic field, $H^* \approx 4$ kOe). This amounts to stating

*Electronic address: santoshkumar@phy.iitb.ac.in

†Present address: Department of Physics, Indian Institute of Science Education and Research Bhopal, Bhopal 462066, India.

‡Electronic address: arunkgrover@gmail.com

that the vortex matter created in the field-cooled mode (FC) below H^* exhibits better spatial ordering than that obtained in the zero field-cooled manner. This feature also is in sharp contrast to the behavior [19–22] seen at the higher fields, where one encounters order-disorder transition (*a la* PE phenomenon). The vortex matter created via field-cooling is expected to be spatially more disordered (than the ZFC state) due to supercooling of an amorphous vortex matter below the PE region. We present evidences that H^* signifies a crossover regime from an ordered BG phase into a disordered amorphous phase while reducing the field.

II. EXPERIMENTAL DETAILS

Single crystals of $\text{Yb}_3\text{Rh}_4\text{Sn}_{13}$ have been grown by tin flux method [23]. The specimen chosen for the present study is platelet shaped, with a planar area of 5.76 mm^2 and thickness of 0.62 mm . The superconducting transition temperature (T_c) of this crystal is found to be nearly 7.5 K . Magnetization data, both ac as well as dc, were recorded using the same instrument, viz., Superconducting Quantum Interference Device-Vibrating Sample Magnetometer (SQUID-VSM, Quantum Design Inc., USA). The magnetic field was directed along the crystalline [110] axis, with a possible error in the alignment to be within 5° . The demagnetization factor in this orientation is expected to be small as the field is applied in the plane of the thin platelet, i.e., normal to the smallest dimension (thickness) of the sample. In the dc measurements, we kept the amplitude of vibration of the sample to be small ($\approx 0.5\text{ mm}$) so as to minimize the field-inhomogeneity along the scan length. During the ac susceptibility measurements ($\chi'(H, T)$), an ac field of amplitude 1 Oe and frequency 211 Hz was superimposed on the applied dc field.

III. RESULTS

A. Isothermal dc M - H loops: Manifestation of the peak effect phenomenon

The inset panel of Fig. 1(a) displays the first two quadrants of an isothermal dc magnetization hysteresis loop (M - H) obtained at $T = 2\text{ K}$ for field applied parallel to the [110] plane of $\text{Yb}_3\text{Rh}_4\text{Sn}_{13}$ crystal. The $M(H)$ curve can be seen to be hysteretic between the forward ($M(H^+)$) and the reverse ($M(H^-)$) sweeps of the magnetic field, as expected for a pinned type-II superconductor. However, there exists an unusual enhancement in the hysteresis width ($\Delta M(H) = M(H^+) - M(H^-)$) prior to H_{c2} , as apparent from the encircled portion of the $M(H)$ curve. A magnified view of this portion is displayed on an expanded scale in the main panel of Fig. 1(a). Using a prescription of the Bean's Critical State Model [24], Fietz and Webb have shown [25] that the hysteresis width

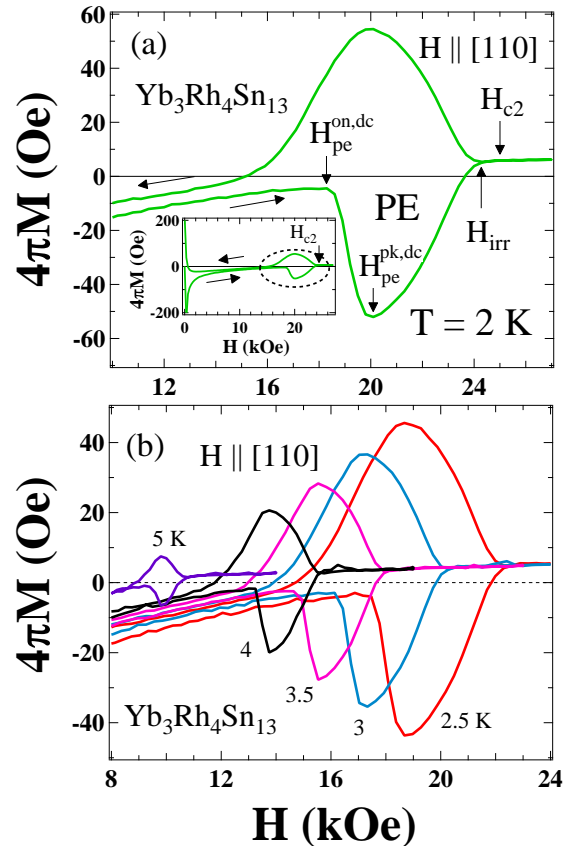


Figure 1: (Color online) (a) An expanded portion of (isothermal) dc M - H loop at $T = 2\text{ K}$ demonstrating a typical PE phenomenon in a single crystal of $\text{Yb}_3\text{Rh}_4\text{Sn}_{13}$. The inset displays the first two quadrants of this loop in the entire field range of investigation, i.e., $0 < H < 28\text{ kOe}$. (b) The M - H curves at different temperatures show the evolution of the PE feature as it occurs at different fields.

(ΔM) can be taken as a measure of the critical current density, $j_c(H, T)$. Therefore, the enhancement in ΔM reflects an unusual increase in $j_c(H)$ a little below H_{c2} , which can be identified as the PE phenomenon. The onset field ($H_{pe}^{on,dc}$) and the peak field ($H_{pe}^{pk,dc}$) of the PE stand located in the main panel of Fig. 1(a). The merger of $M(H^+)$ and $M(H^-)$ beyond the bubble feature identifies the irreversibility field (H_{irr}).

We show in Fig. 1(b), the fingerprint of PE feature at different temperatures, as indicated. On increasing the temperature, a systematic decrease in the onset and the peak field values of the PE is well apparent. The decrease in $H_{pe}^{on,dc}$ and $H_{pe}^{pk,dc}$ with T , nearly following the variation of H_{c2} with T , is a characteristic feature of the PE phenomenon. The order-disorder transition pertaining to PE has been argued to have first-order character, as was well evident in the results of small angle neutron scattering study in a low T_c superconductor Nb [17] and those of scanning Hall probe microscopy in 2H-NbSe_2 [26].

B. Isothermal ac susceptibility $\chi'(H)$ responses: Identification of an additional anomaly in conjunction with the PE phenomenon

To investigate further the order-disorder transition(s) in the vortex matter, we recorded the isothermal ac susceptibility ($\chi'(H)$) responses as shown in Fig. 2. The sample was initially cooled-down to a chosen temperature in (near) zero field and thereafter the χ' data were recorded while ramping the field to higher values. The $|\chi'|$ values at $T = 2$ K can be seen to fall monotonically with increasing field until about a certain field, marked as $H_p^{on,ac}$ (≈ 12.5 kOe, cf. main panel of Fig. 2(a)). Above $H_p^{on,ac}$, a broad (anomalous) dip-like feature encompassing a large field interval (i.e., $H_p^{on,ac} < H < H_{c2}$) can be noticed. Note that the identification of onset field ($H_p^{on,ac}$) of this dip feature was made possible by locating the first zero-crossing in the derivative plot of $\chi'(H)$ as

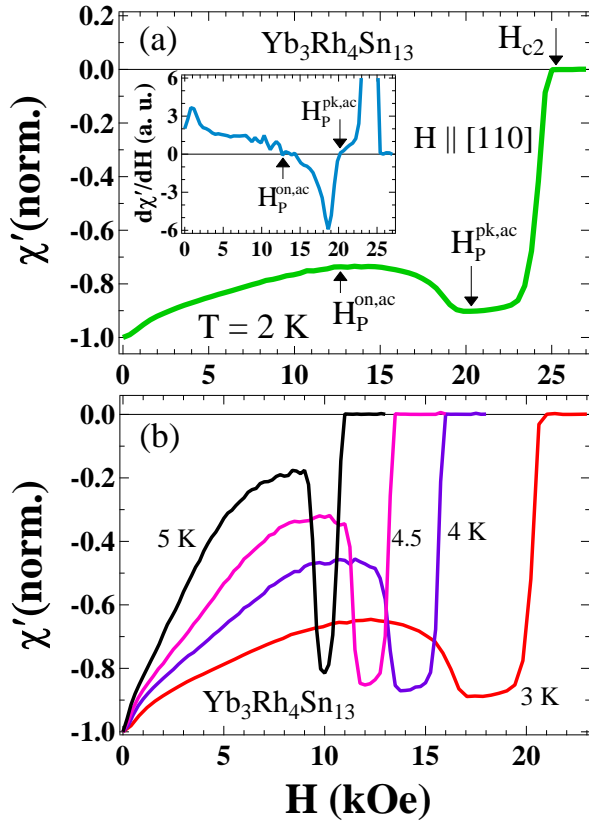


Figure 2: (Color online) (a) The real part of (isothermal) ac susceptibility ($\chi'(H)$) data plotted against the dc magnetic field at $T = 2$ K. A broad dip-like anomaly triggering at a field marked as $H_p^{on,ac}$ has been observed. The inset panel illustrates a portion of $d\chi'/dH$ curve at $T = 2$ K which helps to identify the onset ($H_p^{on,ac}$) and peak ($H_p^{pk,ac}$) positions of the anomaly identified respectively via the first and second zero-crossings of the derivative plot. (b) $\chi'(H)$ curves at different temperatures show how the anomaly changes from a broad to a narrow one with increase in temperature.

displayed in an inset panel of Fig. 2(a). The second zero-crossing in $d\chi'/dH$ identifies the peak position (marked as $H_p^{pk,ac}$) of the anomalous variation in $\chi'(H)$ across the dip region. We recall here that the χ' value reflects j_c through the two relations [27], (i) $\chi' \sim -1 + \alpha h_{ac}/j_c$ for $h_{ac} < h^*$ and (ii) $\chi' \sim -\beta j_c/h_{ac}$ if $h_{ac} > h^*$, where α and β are size and geometry dependent factor, h_{ac} is the amplitude of the ac field and h^* is the ac field for full penetration. Following equation (i), the anomalous variation in $\chi'(H)$ above $H_p^{on,ac}$ in Fig. 2(a) amounts to an unusual increase in otherwise monotonically decreasing $j_c(H)$. Similar anomalous behaviour in $\chi'(H)$ can also be observed at different temperatures as illustrated in Fig. 2(b). While the dip feature remains quite broad at lower temperatures, one can note that the width of this anomalous region gets substantially reduced on higher temperature side. For example, the dip in $\chi'(H)$ at 5 K is observed to be much sharper with a narrow transition width (of nearly 2 kOe) prior to approaching H_{c2} which, following equation (ii), amounts to a rapid increase in $j_c(H)$ echoing the characteristics of the quintessential PE phenomenon.

A comparison of $\chi'(H)$ data presented in Fig. 2(a) with that of the $M-H$ loop shown in Fig. 1(a), tells us that the peak field value ($H_p^{pk,ac} \approx 20$ kOe) of the anomaly observed in the former is nearly the same as the corresponding peak field value ($H_{pe}^{pk,dc}$) of the PE observed at the same temperature in the latter. However, if we seek the analog of onset field of the anomaly seen in ac $\chi'(H)$, viz., $H_p^{on,ac}$ (≈ 12.5 kOe, Fig. 2(a)), we find that no anomalous feature stands depicted at this field value in the dc $M-H$ loop (cf. Fig. 1(a)). This implies an additional anomaly has got unearthed (at $H_p^{on,ac}$) in the $\chi'(H)$ scans in the specimen of $Yb_3Rh_4Sn_{13}$ which is not observed in its $M-H$ runs. To seek the rationalization of this discrepancy in the ac and dc magnetization data, one can consider the presence of an ac driving force inevitably superimposed on the dc field during the $\chi'(H)$ runs as an important difference between the two sets of measurements. Two important factors in conjunction, viz., (i) the shaking effect of an ac driving force on the vortex matter and, (ii) driving effect due to a continuous ramping of the dc magnetic field, may be acting as a combined driving force leading to the triggering of additional anomaly in $\chi'(H)$ runs. To shed some more light onto this assertion, it became tempting to explore the isofield ac susceptibility responses, where an effect due to the ramping of magnetic field would not be present. These are described ahead.

C. Isofield ac susceptibility $\chi'(T)$ responses: identification of the PE phenomenon

Figure 3 displays the temperature dependences of the in-phase ac susceptibility ($\chi'(T)$) obtained at various fixed dc fields. The sample was initially cooled down to 1.8 K in (nominal) zero field, a desired field was then ap-

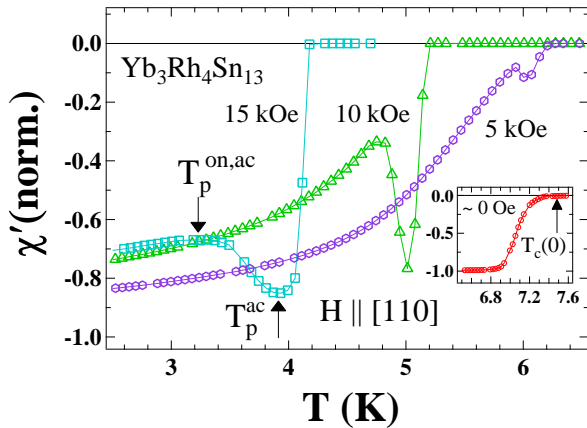


Figure 3: (Color online) Observation of PE anomaly in temperature-dependent ac susceptibility ($\chi'(T)$) runs at various fixed dc fields. Onset ($T_p^{on,ac}$) and peak (T_p^{ac}) temperature of PE have been marked in the $\chi'(T)$ curve for $H_{dc} = 15$ kOe. The inset shows the occurrence of zero-field superconducting-normal transition at $T \approx 7.5$ K.

plied and the $\chi'(T)$ data were recorded while warming up to higher temperatures ($T > T_c$). The zero-field superconducting transition temperature, $T_c(0)$ identified via the onset of diamagnetic response is found to be about 7.5 K (cf. inset panel of Fig. 3). Fingerprint of the PE feature identified by a dip-like characteristic can be observed in all the curves shown in the main panel of Fig. 3. At $H = 5$ kOe, the dip in $\chi'(T)$ is found to be less prominent, however, it evolves into a sharp (negative) peak at higher field values (see, e.g., $\chi'(T)$ response in $H = 10$ kOe). On further increasing the field to 15 kOe, the PE region becomes broad, which is apparent from a wider gap between the onset ($T_p^{on,ac}$) and the peak (T_p^{ac}) temperatures of the PE marked in the main panel of Fig. 3. Such a broadening seen in the PE feature at higher fields may be ascribed to effects of an enhancement in ‘effective pinning’ with field, as articulated by Giamarchi and Le Doussal [1, 2] and elucidated in a crystal of low T_c superconductor 2H-NbSe₂ by Banerjee *et al.*, [21].

A lesser developed (PE) anomaly at lower field value (~ 5 kOe) suggests the possibility of a lesser ordered vortex matter emerging at that end as well. Such a trend is consistent with the notion that an ordered vortex lattice (Bragg glass) undergoes a transition into a disordered phase on lowering the field [28, 29].

Across the field interval from about 5 kOe to 14 kOe, the vortex matter seems to evolve into a better spatially ordered (Bragg glass) phase, as is evidenced by a sharp PE feature at 10 kOe in Fig. 3.

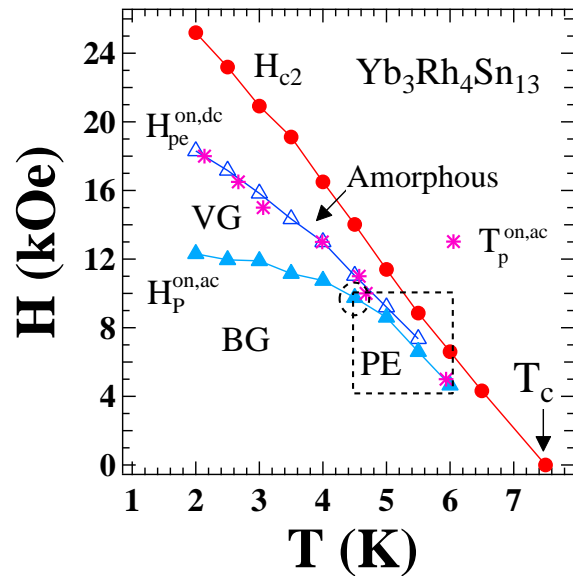


Figure 4: (Color online) A sketch of vortex phase diagram in our crystal of $\text{Yb}_3\text{Rh}_4\text{Sn}_{13}$. $H_p^{on,ac}(T)$ and $H_{pe}^{on,dc}(T)$ have been extracted from $\chi'(H)$ and $M-H$ plots, respectively. Below $T = 4.5$ K, the former resembles the BG to VG transition line (refer text in section-4, ‘Discussion’) while the latter portrays the characteristics of onset of the PE anomaly. In the boxed-region, both $H_p^{on,ac}(T)$ and $H_{pe}^{on,dc}(T)$ lines behave as the onset of the PE transition. The onset temperatures ($T_p^{on,ac}(H)$) of the PE obtained from isofield $\chi'(T)$ scans almost fall on the onset field values $H_{pe}^{on,dc}(T)$ of the PE extracted from $M-H$ loops. $H_{c2}(T)$ taken from $M-H$ loops depicts usual linear fall with increase in temperature.

D. $H-T$ phase diagram

It is instructive to compare the results of ac and dc magnetization data of Figs. 1 to 3. For this purpose, we present in Fig. 4, a $H-T$ phase diagram of $\text{Yb}_3\text{Rh}_4\text{Sn}_{13}$, which comprises the field/temperature values corresponding to the onset positions of the anomalies seen in Figs. 1 to 3. The following features in this phase diagram are noteworthy:

1. The onset field values ($H_{pe}^{on,dc}(T)$) of the PE (open triangles) acquired from the $M-H$ data (Fig. 1) fall smoothly with the increase in temperature, a trend similar to the $H_{c2}(T)$ line.

2. The corresponding onset field values ($H_p^{on,ac}(T)$) shown by closed triangles) of the anomaly observed in $\chi'(H)$ plots (Fig. 2), however, do not coincide with the onset position ($H_{pe}^{on,dc}(T)$) of the PE over a significantly large portion of the $H-T$ space (i.e., $T < 4.5$ K). Here, the $H_p^{on,ac}(T)$ line stays substantially below the $H_{pe}^{on,dc}(T)$ line. Moreover, $H_p^{on,ac}(T)$ values exhibit a weaker temperature dependence at temperatures below 4.5 K unlike the faster temperature dependence seen in case of $H_{pe}^{on,dc}(T)$. The two onset field lines, $H_{pe}^{on,dc}(T)$

and $H_p^{on,ac}(T)$, come closer to each other only in the boxed region (i.e., at $T > 4.5$ K and $5 \text{ kOe} < H < 10 \text{ kOe}$) and show identical temperature dependence.

3. The discrepancy in the phase diagram (Fig. 4) pertaining to the location of the onset fields of the anomalies seen in the (isothermal) M - H and $\chi'(H)$ data prompts the need to take into consideration the results of isofield $\chi'(T)$ scans (Fig. 3) as well. For this purpose, we have plotted in the phase diagram the onset temperatures ($T_p^{on,ac}(H)$) of the PE (shown by stars) obtained from $\chi'(T)$ scans. It is curious to note that the $T_p^{on,ac}(H)$ values fall almost on the onset field ($H_{pe}^{on,dc}(T)$) line of the PE transition. *We draw an important inference here that the results of isothermal dc M - H loops and the isofield ac $\chi'(T)$ scans predict the onset of the PE anomaly at nearly the same phase boundary, i.e., ($H_{pe}^{on,dc}$, $T_p^{on,ac}$) line.*

Clearly, there exists an additional anomaly (apart from the PE) located deeper (at $H_p^{on,ac}(T)$) in the mixed state of $\text{Yb}_3\text{Rh}_4\text{Sn}_{13}$, which has got unveiled only from the outcomes of the $\chi'(H)$ data. The other two measurement techniques (viz., the M - H and $\chi'(T)$ scans), on the other hand, reveal the fingerprints of only one kind of anomaly, i.e., the PE. This corroborates our previous assertion that both an ac driving force as well as the dc magnetic field ramping together trigger the said additional anomaly well below the onset of PE (these two factors not being present together during the individual dc M - H and ac $\chi'(T)$ runs).

The lowest field down to which the PE could be discernible in Fig. 4 is nearly 4.5 kOe. Since there is hardly any fingerprint of PE feature below this value, we could surmise that the vortex matter there may be disordered. This proposition is explored further via the thermomagnetic history-dependent magnetization measurements.

E. Thermomagnetic history dependence in $j_c(H, T)$: FC state is more ordered than the ZFC at low fields

Figure 5 displays the shielding responses ($\chi'(H)$) obtained at 2 K for the system prepared in two different histories, viz., zero field-cooled (ZFC) and field-cooled (FC) modes. The isothermal $\chi'(H)$ data in the ZFC mode (open circles) are the same as that presented in Fig. 2(a). In the FC case, the sample was first cooled from normal state ($T > T_c(0)$), in the presence of a certain applied field ($H < H_{c2}$) down to $T = 2$ K and a given $\chi'(H)$ value was recorded. Thereafter, the sample was warmed up again to a higher $T (> T_c(0))$ and the same procedure was followed for recording another χ'_{FC} value in a different cooling field. A collation of such $\chi'_{FC}(H)$ data at 2 K is illustrated (closed circles) in Fig. 5. Three different field intervals can be identified; (I) Across the range, $4 \text{ kOe} < H < H_p^{pk,ac}$, the ZFC and FC curves can be seen to be well separated with the latter possessing more diamagnetic values than the former. Fol-

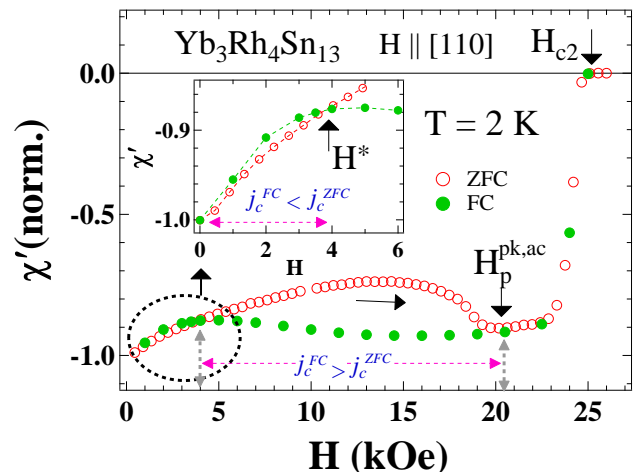


Figure 5: (Color online) A comparison of $\chi'(H)$ plots recorded in ZFC and FC modes at $T = 2$ K. Across the field range $4 \text{ kOe} < H < H_p^{pk,ac}$, the FC state is more diamagnetic than the ZFC, implying the inequality, $j_c^{FC} > j_c^{ZFC}$. A reversal of this situation, i.e., $j_c^{FC} < j_c^{ZFC}$ is observed below 4 kOe ($\sim H^*$) in an expanded portion of $\chi'(H)$ as shown in the inset panel.

lowing equations (Ref. [27]) (i) $\chi' \sim -1 + \alpha h_{ac}/j_c$ and (ii) $\chi' \sim -\beta j_c/h_{ac}$, a more negative χ' implies larger j_c . Therefore, in the field interval $4 \text{ kOe} < H < H_p^{pk,ac}$, the FC state exhibits a higher j_c than that in the ZFC state (i.e., $j_c^{FC} > j_c^{ZFC}$). As per a description of Larkin-Ovchinnikov collective pinning theory [30, 31] for weakly-pinned superconductors, j_c relates inversely to the volume (V_c) of a domain within which the vortices are collectively pinned and remain well correlated. Therefore, a higher j_c amounts to a smaller V_c , and hence signifies a more (strongly-pinned) disordered vortex matter. (II) The history-dependence in $j_c(H)$ tends to cease above $H_p^{pk,ac}$ as we observe the two curves to overlap there. This is in line with the understanding that the vortex matter above the peak field of the PE is generally believed to be 'disordered in equilibrium' [17]. (III) The ZFC and FC curves appear to overlap at low fields ($H < 4 \text{ kOe}$) as well, as apparent from the two sets of data points in the encircled portion of $\chi'(H)$ (cf. main panel of Fig. 5). However, a closer examination of the two $\chi'(H)$ curves in this region on an expanded scale (see inset panel of Fig. 5) reveals slightly less diamagnetic values (at a given H) for the FC state than that for the ZFC mode, which implies the reversal of the above inequality; i.e., $j_c^{FC} < j_c^{ZFC}$ for $H < 4 \text{ kOe}$. We have marked this crossover field value ($\sim 4 \text{ kOe}$) as H^* in the inset panel of Fig. 5. Such an inequality ($j_c^{FC} < j_c^{ZFC}$) below H^* is found to be very robust as it can be observed at other temperatures as well (all data not shown here but the H^* values at different temperatures have been displayed in the H - T phase diagram as shown ahead in Fig. 8).

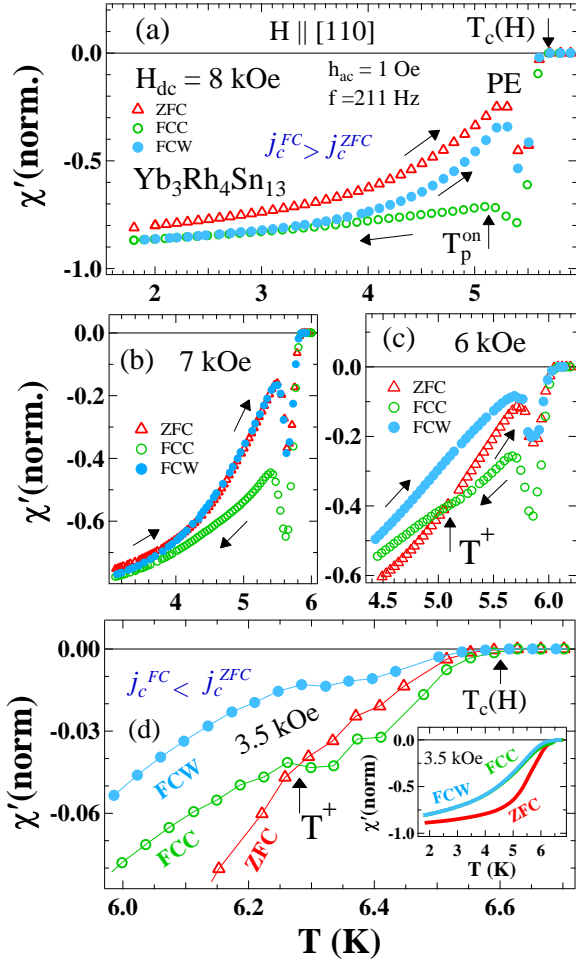


Figure 6: (Color online) Temperature-dependent $\chi'(T)$ curves obtained in ZFC, FCC and FCW modes at $H_{dc} =$ (a) 8 kOe, (b) 7 kOe, (c) 6 kOe and (d) 3.5 kOe. At higher fields (8 kOe, panel (a)), the FC curves (FCC and FCW) are more diamagnetic than the ZFC and hence, they imply the inequality $j_c^{FC} > j_c^{ZFC}$. On reducing the field to 6 kOe (panel (c)) and then to 3.5 kOe (inset panel of (d)), the ZFC curve becomes the most diamagnetic below a characteristic temperature T^+ (i.e., $j_c^{FC} < j_c^{ZFC}$). At $H = 3.5$ kOe (see main panel of (d)) there is no signature of PE in the ZFC mode while a residual fingerprint of it can be seen in the FC curves.

The H - T phase space region below H^* was further explored via isofield $\chi'(T)$ scans recorded in different modes, viz., zero field-cooled (ZFC), field-cooled cool-down (FCC) and field-cooled warm-up (FCW) runs as depicted in Fig. 6. The sample was cooled in (near) zero field from the normal state down to 1.8 K, and then a desired magnetic field was applied. Thereafter, the $\chi'(T)$ data were obtained (marked as ZFC in Fig. 6), while warming the sample to higher T . Following this, $\chi'(T)$ data were again recorded while cooling the sample down to 1.8 K (marked as FCC) in the presence of the same applied field, and thereafter while warming it towards the normal state (marked as FCW). At $H = 8$ kOe

(Fig. 6(a)), the shielding response is found to be less diamagnetic for the ZFC case than that observed for the FCC and FCW modes (i.e., $j_c^{FC}(8 \text{ kOe}) > j_c^{ZFC}(8 \text{ kOe})$ at all temperatures). This implies that the vortex matter created in the ZFC mode is better spatially ordered among the three modes which is consistent with the observations made at this field value in Fig. 5. At a lower field ($H = 7$ kOe), the ZFC curve nearly overlaps with the FCW; these two curves stay less diamagnetic than the FCC for $T > 4$ K (cf. Fig. 6(b)). On reducing the field further to 6 kOe (Fig. 6(c)), the FCW curve can now be seen to be the least diamagnetic amongst the three curves at all temperatures. Further, there is an unusual intersection of ZFC and FCC curves at a certain temperature marked as T^+ , below which the ZFC is now more diamagnetic than the FCC and FCW curves. The ZFC curve at a lower field of 3.5 kOe (see inset panel of Fig. 6(d)) can be seen to be more diamagnetic and well separated from the other two (FCC and FCW) curves. This would imply the inequality $j_c^{FC} < j_c^{ZFC}$, which, in turn, suggests that the vortex matter created in the ZFC mode is more disordered than that created in the FC mode. This situation is the reversal of that depicted in Fig. 6(a) and is in agreement with the conclusion drawn from the history-dependent $\chi'(H)$ responses below $H^* \approx 4$ kOe (cf. Fig. 5). An expanded portion of $\chi'(T)$ plots at $H = 3.5$ kOe in the main panel of Fig. 6(d) shows that the fingerprint of PE ceases to exist in the ZFC mode, whereas a tiny modulation can still be noticed across $T^+ < T < T_c(H)$ in the case of FCC and FCW runs. This suggests that the vortex state created in ZFC manner at $H = 3.5$ kOe is disordered to such an extent that any order-disorder vortex phase transition may not be identifiable in the temperature-dependent warm-up measurements. On the other hand, at the same field value (3.5 kOe), a nascent signature *à la* PE observed in FCC and FCW modes suggests that vortex matter is comparatively better ordered when created in the FC mode at 3.5 kOe.

Another demonstration of a more ordered FC state (than the ZFC state) at lower field values is apparent from the results of thermomagnetic history-dependent dc M - H measurements, as illustrated in Fig. 7. The M - H curve shown by open circles pertains to the usual hysteresis loop obtained in the ZFC mode at $T = 2$ K. Magnetization data recorded in the FC mode (M_{FC}), i.e., after cooling the sample from a higher T ($> T_c(0)$) down to 2 K in the presence of different chosen field values have also been displayed by open triangle data points in Fig. 7(a). If we associate the M_{FC} values to the equilibrium (reversible) magnetization (M_{eq}) and ignore the contribution due to bulk currents that can get set up due to a gradient in macroscopic field (H) (as in the case of ZFC), then, as per equation $M_{eq} = (M(H^+) + M(H^-))/2$ [25], the M_{FC} data are supposed to fall in the middle of the ZFC envelope loop (as, for example, evident in Ref. [10]). Figure 7(a) depicts an unexpected scenario, wherein the M_{FC} data points stay

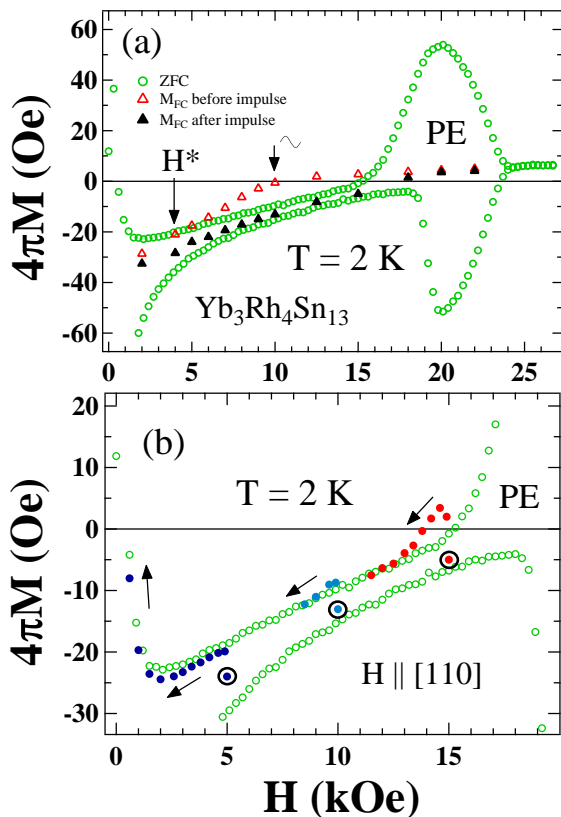


Figure 7: (Color online) (a) M - H loop at $T = 2\text{ K}$ in the ZFC mode (open circles). The field-cooled magnetization values (M_{FC} , open triangles) for $5\text{ kOe} < H < 15\text{ kOe}$ unexpectedly lay outside the ZFC envelope loop. An impulse of an ac field (amplitude = 10 Oe , $f = 211\text{ Hz}$) imposed on the FC states created at different H (open triangles) leads the M_{FC} values to fall well within the loop (closed triangles). (b) Minor hysteresis loops at $T = 2\text{ K}$ traced while reducing the field to zero after creating the FC states at $H = 5, 10, 15\text{ kOe}$ and imposing an ac field impulse on them.

outside the envelope hysteresis loop for field (H) values in the interval, $5\text{ kOe} < H < 15\text{ kOe}$. We can try to rationalize this using a model due to Clem and Hao [32] which accounts for the FC magnetization of a type-II superconductor when a gradient in macroscopic field gets established as a consequence of flux expulsion during the FC mode. In such a situation, the M_{FC} values deviate from M_{eq} (ideal case of no flux-pinning). This deviation of FC magnetization from M_{eq} values is indeed anticipated to be governed by the strength of bulk pinning at a given field; the extent of deviation is more (less) for stronger (weaker) pinning strength (j_c) (see Fig. 5 in Ref. [32]). The M_{FC} values (see open triangles, Fig. 7(a)) falling outside the envelope loop in the present case, for $H > 5\text{ kOe}$ are due to a larger j_c value associated with the vortex matter created in the FC mode and the flux density gradient [32] that gets set-up while field-cooling. Note that below $H = 5\text{ kOe}$ (close to $H^* \sim 4.5\text{ kOe}$), the

FC state seems to have a lower j_c value (better ordered) as the M_{FC} value here remains well within the envelope (i.e., nearer to M_{eq}).

As a further experimentation, on each occasion, after a FC state was created at a chosen field value, we momentarily perturbed it with an ac field impulse of amplitude 10 Oe at a frequency of 211 Hz (applied for about 6 seconds). It is curious to note that the magnetization recorded after the impulse treatment (closed triangles data points in Fig. 7(a)) fall well within the envelope loop. It appears as if the magnetization response of a FC state after perturbation by an impulse conforms to the anticipated respective equilibrium value (M_{eq}) (closed triangles data points) located in the middle of the ZFC envelope loop. The imposition of an ac field impulse results in the reconfiguration of an unperturbed FC state into state, comparison of whose j_c value with that of the corresponding ZFC state can be very instructive. We thus recorded the 'FC minor hysteresis loops'. Figure 7(b) shows the magnetization curve obtained while reducing the dc field to zero after the (perturbed) FC states were created (encircled) at $H = 5\text{ kOe}$, 10 kOe and 15 kOe . The initial magnetization value recorded while decreasing the field from $H = 5\text{ kOe}$ undershoots the ZFC envelope, and the magnetization curve thereafter traverses a path that remains within the envelope loop as the field is ramped down to the zero value. Taking cue from the linear relation between hysteresis width and j_c [25], the (perturbed) FC state is reckoned to have a lower j_c value than that in the ZFC for fields below H^* . This observation fortifies the inferences drawn from data in Figs. 5 and 6. At $H = 10\text{ kOe}$, the magnetization data, while reducing the field, first overshoots the ZFC envelope though marginally, and thereafter it retraces the reverse leg ($M(H^-)$) of the ZFC magnetization curve. It can be argued that the FC state here exhibits j_c value slightly higher than that in the corresponding ZFC states. A significant overshooting of the ZFC envelope loop is witnessed at a higher field of 15 kOe , which indicates a larger j_c value for the FC state than that created in the ZFC mode. Note that the field value of 15 kOe lies in the anomalous region, $H_p^{on,ac}(T) < H < H_{pe}^{on,dc}(T)$ of the H - T space at 2 K (Fig. 4) which, as discussed in section-IV ahead, is 'partially disordered in equilibrium' as the multi-domain VG state.

IV. DISCUSSION

The magnetization measurement techniques (both ac and dc) employed in the present work have lead to new revelations in $\text{Yb}_3\text{Rh}_4\text{Sn}_{13}$ which have been summarized in the form of a modified H - T phase diagram in Fig. 8. These include, (i) the occurrence of a broad anomaly located deeper in the mixed state triggering at $H_p^{on,ac}(T)$ line as seen in the $\chi'(H)$ curves (Fig. 2), (ii) identification of onset position of the PE at $H_{pe}^{on,dc}$, $T_p^{on,ac}$ line as obtained from both the dc M - H (Fig. 1) and the ac

$\chi'(T)$ (Fig. 3) plots, and (iii) a characteristic line $H^*(T)$ extracted from Fig. 5, below which a vortex matter created in the FC mode is somewhat more ordered than that obtained in the ZFC manner. Following a description of L-O theory [30, 31], we argue that the anomaly in $\chi'(H)$ (Fig. 2) reflects a shrinkage in V_c as $j_c \propto 1/\sqrt{V_c}$ and hence, can be termed as an order-disorder transition in the vortex matter. Note that the L-O theory is well applicable for weakly-pinned superconductors as in the present case of $\text{Yb}_3\text{Rh}_4\text{Sn}_{13}$ (ratio of depinning and depairing current densities is of the order of 10^{-4}). The location of $H_p^{on,ac}(T)$ line deeper in the mixed state and its weak temperature-dependence outside the boxed region in Fig. 4 can be argued to relate to the disorder-induced transition [1, 2, 6, 7] of a quasi-ordered (elastic) vortex lattice *à la* BG phase to the dislocation-mediated (multi-domain) VG phase. Note that the peak field of the anomalous variation in $j_c(H)$ as reflected in dc $M-H$ and ac $\chi'(H)$ plots, viz., $H_{pe}^{pk,dc}(T)$ (closed squares) and $H_p^{pk,ac}(T)$ (open squares), is consistent, as the two sets of data points extracted from two different measurements can be seen to be overlapping in Fig. 8. This would imply that the complete amorphization of the vortex matter (which is generally believed to occur at peak field of the PE [21]) occurs at the same field/temperature value while performing measurements via ac and dc magnetization techniques.

It has been shown earlier that the annealing effects on the vortex matter, produced either by an ac driving force [17, 33] or by repeated cycling of the dc magnetic field [34, 35], eliminate either partly or completely a (metastable) disordered vortex phase yielding an ordered vortex configuration. Also, the residual presence of a disordered (metastable) vortex phase usually governs the onset position of the order-disorder (PE) transition(s) [21, 29, 36]. As a usual behavior, the onset position of the PE shifts to higher field values after the annealing of (disordered) vortex phase, whereas the same moves to lower fields when the amount of quenched disorder is larger [21, 29]. Surprisingly, the shaking effect of an ac driving force appears to be counterintuitive in the present study, as it promotes the spatial disordering of the vortex matter rather than its usual role of improving the state of spatial order. This is well apparent by the (early) occurrence of an order-disorder transition at $H_p^{on,ac}(T)$ line (cf. Fig. 8) in the $\chi'(H)$ runs which involve the ac drive. In the absence of an ac driving force as in dc $M-H$ scans, the onset of order-disorder transition (PE) is seen at higher fields; $H_{pe}^{on,dc}(T)$ values in Fig. 8 are located significantly above the BG to VG transition ($H_p^{on,ac}(T)$) line. If one assumes that the shaking effect on the vortex array by an ac drive results in the lowest equilibrium-like state of the system (as in Ref. [17]) under given circumstances, then the region bounded by the phase lines, $H_p^{on,ac}(T)$ and $H_{pe}^{on,dc}(T)$, in Fig. 8 can be accepted as “disordered in equilibrium” in the form of multi-domain vortex glass phase. The present findings echo similar assertions made recently by us [18] in another study in a single crystal of

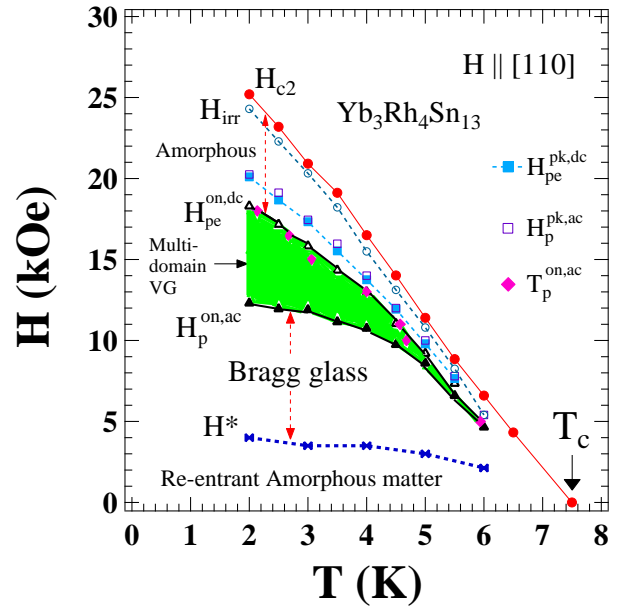


Figure 8: (Color online) Complete vortex phase diagram in our crystal of $\text{Yb}_3\text{Rh}_4\text{Sn}_{13}$. Various regions have been identified (refer text for details). A delineation between the BG to VG transition (occurring at $H_p^{on,ac}(T)$) and the PE anomaly (at $H_{pe}^{on,dc}(T)$), is well apparent. The peak field values $H_{pe}^{pk,dc}(T)$ and $H_p^{pk,ac}(T)$ obtained respectively from the $M-H$ and $\chi'(H)$ data almost fall on the same phase boundary. The region between ($H_{pe}^{pk,dc}(T)/H_p^{pk,ac}(T)$) and the $H_{irr}(T)$ line presumably comprises pinned amorphous matter while the narrow space between $H_{irr}(T)$ and $H_{c2}(T)$ may involve an unpinned amorphous vortex matter. Below $H^*(T)$ (obtained from Fig. 5), the $H-T$ phase space region comprises (reentrant) disordered vortex matter, a vortex configuration created here in the FC manner is found to be slightly more ordered than that in the ZFC mode.

a low T_c superconductor, $\text{Ca}_3\text{Ir}_4\text{Sn}_{13}$. However, in that study in $\text{Ca}_3\text{Ir}_4\text{Sn}_{13}$, a distinct demarcation between the BG to VG transition line and the locus of the onset of the PE anomaly in its vortex phase diagram was not apparent, which has now been clearly sorted out in the phase diagram of $\text{Yb}_3\text{Rh}_4\text{Sn}_{13}$.

The nature of BG to VG transition had been argued to be of first-order [37] in a high T_c superconductor. To fortify this proposition, we may emphasize that the region bounded between $H_p^{on,ac}(T)$ and $H_{pe}^{on,dc}(T)$ in Fig. 8 which is shown from the $\chi'(H)$ data to be disordered in equilibrium is indeed an ordered vortex phase when viewed from the outcomes of the dc $M-H$ measurements. Therefore, vortex phase in this region can be treated as a superheated ordered BG phase. This attests the first-order nature of the BG to VG transition in a low T_c superconductor.

The change in magnetic field tunes the inter-vortex spacing which, in turn, can influence the balance between the strength of vortex pinning and the (elastic) interac-

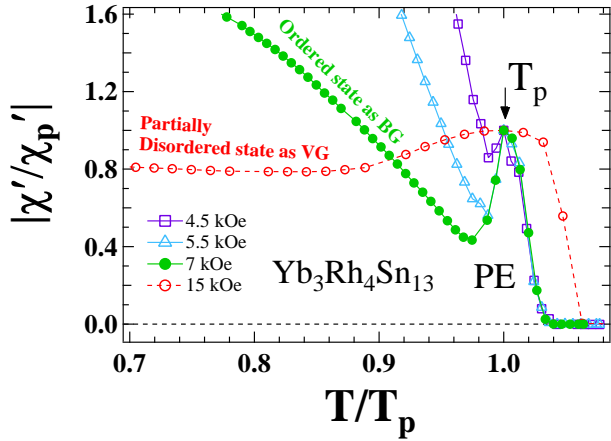


Figure 9: (Color online) $|\chi'/\chi'_p|$ data (normalized with respect to χ' value at peak position of the PE) plotted against the reduced temperature, T/T_p at various constant dc fields. The shape of the PE anomaly changes with field. At $H = 4.5$ kOe, there is a tiny peak feature while a much prominent peak feature can be noticed at a higher field, $H = 7$ kOe. The PE feature gets broadened at a further elevated field of 15 kOe.

tions between the vortices. As a result, the extent of spatial ordering/disordering in the vortex matter may vary in different regions of the H - T phase space. Further, an enhancement in effective pinning at a given field value can give rise to a qualitative change in the evolution of the size of the Larkin domain [30, 31], as had been experimentally demonstrated [38] via the evolution of PE feature in the isofield $\chi'(T)$ measurements in crystal(s) of 2H-NbSe₂. Motivated by this, we shall now examine how the PE feature evolves with magnetic field in the case of our crystal of Yb₃Rh₄Sn₁₃. We show in Fig. 9 the normalized $|\chi'/\chi'_p|$ plots (χ'_p corresponds to χ' value at peak position of PE where vortex matter is most disordered for a given inter-vortex spacing and the underlying quenched random disorder) against the reduced temperature = T/T_p , (T_p is peak temperature of PE obtained in the ZFC mode for various fixed fields). The PE feature remains absent at fields below $H = 4.5$ kOe (data not shown here), which may be because of a disordered vortex matter prevailing there. Note that the larger inter-vortex spacings at low flux density results in weaker interaction between the vortices to counter disordering influence of the pinning centres. The vortex configuration created at low fields ought to be highly disordered akin to the reentrant amorphous vortex matter anticipated in earlier studies [39–42]. With the increase in field, the interaction effects strengthen and consequently, a sparse disordered vortex configuration can progressively change into an ordered one, as has been demonstrated earlier in Refs. [43, 44]. This is apparent from Fig. 9 by the appearance of a tiny PE feature firstly at $H = 4.5$ kOe. A more pronounced signature of PE occurring at $H = 5.5$ kOe

suggests further improvement in the spatial ordering of vortex matter with the increase in field prior to the onset of PE. At a higher field of 7 kOe, there emerges a very well developed PE feature, which is indicative of a well-ordered vortex (BG) phase prevailing prior to the onset of the PE transition at this field value. A different scenario is, however, depicted at a higher field, $H = 15$ kOe, wherein the order-disorder transition can be seen to be much broader. We surmise that the vortex phase prior to the order-disorder transition at this field value is partially disordered (*à la* multi-domain VG phase) so that any order-disorder transition would reflect a lesser shrinkage in V_c (as compared to that at lower fields) or equivalently, lesser increment in j_c [30, 31] associated with this state. In all, the $|\chi'/\chi'_p|$ plots of Fig. 9 have lead us to infer that a disordered vortex phase at low field end ($H < 4.5$ kOe) transforms into an ordered one (BG phase) with increase in field. A further enhancement in field may transform an ordered vortex phase (BG) into a partially disordered (VG) state prior to the onset of PE.

It is useful to recall now a recent study [45] employing the small angle neutron scattering (SANS) technique in another crystal of Yb₃Rh₄Sn₁₃ (which would typically have different amount of quenched random disorder) providing evidences at microscopic level in support of our experimental results. In the SANS study, the evolution of spatial order in vortex matter with vortex lattice spacing (a_0) has been well-depicted by plots of field-dependences of the normalized correlation lengths (both longitudinal, ξ_L/a_0 and transversal, ξ_T/a_0) as well as their ratio (ξ_L/ξ_T) (see Fig. 3 in Ref. [45]). These lengths relate to the longitudinal and radial dimensions of the volume within which the flux lines remain correlated. The full width at half maximum of the rocking curves in longitudinal and transverse directions reflecting the apparent quality of the spatial order and that of the Bragg peaks remains nearly flat in the field interval $5 \text{ kOe} < H < 16 \text{ kOe}$ (cf. Fig. 2 in Ref. [45]). The normalized transversal correlation length (ξ_T/a_0) starts decreasing more rapidly as the field reduces below 4 kOe [45]. Near 4.5 kOe, where we just start to observe the PE feature in $|\chi'(T)|$ scans in our sample, the said ratio has a value ~ 2 [45]. This could imply that when the quality of spatial order in the vortex matter gets more compromised (i.e., $\xi_T/a_0 < 2$), the PE feature would not surface up. The longitudinal correlation length was seen [45] to be nearly fifty times longer than ξ_T . It has been argued [45] that the ratio ξ_L/ξ_T reveals field-induced changes in the parameter $\sqrt{c_{44}/c_{66}}$, where c_{44} and c_{66} are respectively, the tilt and shear moduli of hexagonal vortex lattice. This ratio in their sample remains nearly constant between 5 kOe and 12.5 kOe and starts to fall above it and the rate of decrease becomes very steep above 17 kOe (see inset of Fig. 3(a) of Ref. [45]). Such a trend could be interpreted that the quality of spatial order undergoes a change above about 12.5 kOe and the elasticity of the vortex lattice plummets above 17.5 kOe. In the context of

our sample, this could rationalize that BG to VG transition happens above 12.5 kOe (see Fig. 8). The inset panel in Fig. 3(b) of Ref. [45] shows that the simulated (normalized) vortex-vortex interaction in their sample does not continue to monotonically rise with magnetic field as the inter-vortex spacing progressively decreases with increase in field. The vortex-vortex interaction (for the $\text{Yb}_3\text{Rh}_4\text{Sn}_{13}$ crystal investigated in Ref. [45]) reaches a maximum value near 12 kOe and starts to decrease above about 14 kOe thereby implying that the onset of this decrease is a consequence of notion of enhancement in effective pinning at large field values. Near 20 kOe, the value of the normalized vortex-vortex interaction force for this compound is same as at about 6 kOe [45]. The rapid decrease in this parameter below 5 kOe reflects the dominance of pinning in the field domain of reentrant amorphous state (cf. Fig. 8).

In our present study, the $|\chi'/\chi'_p|$ plots of Fig. 9 summarize the evolution in the spatial order of vortex matter with magnetic field, which ties up well with the results of SANS study [45]. The extent of spatial ordering/disordering in the vortex matter at a given field can be quantified by the ratio of $|\chi'/\chi'_p|$ value just prior to the PE and that at the peak position (see T_p in Fig. 9) of the PE. Note that the correlation length ought to be minimum at the peak (T_p) of the PE and maximum (for a well ordered vortex lattice) just before the PE. In Fig. 9, the said ratio of $|\chi'/\chi'_p|$ at onset and peak positions of the PE can be seen to be increasing smoothly with increasing magnetic field for $4.5 \text{ kOe} < H < 7 \text{ kOe}$, which is consistent with the variation of correlation lengths with field for $H < 10 \text{ kOe}$, as anticipated in Ref. [45]. This would imply that a very well-ordered BG phase emerges nearly at $H = 7 \text{ kOe}$ from a disordered state prevailing below 4.5 kOe. Further, at an elevated field (15 kOe), this ratio decreases substantially as if a transition from the BG phase into a VG like phase has occurred there.

In the end, we draw attention towards the thermomagnetic history effects investigated at lower fields (Figs. 5-7). It is customary to witness a more disordered FC state than the ZFC in the vicinity of the PE phenomenon [19–22]. However, the history-dependent magnetization behavior at lower fields ($H < H^*$) studied here in $\text{Yb}_3\text{Rh}_4\text{Sn}_{13}$ have revealed that the vortex matter in the ZFC mode is more disordered than that in the FC case. The following scenario seems plausible to explain this feature. In the ZFC mode, the injection of vortices at high velocities into a superconducting specimen is influenced by surface barriers and edge effects [46, 47] such that the vortices eventually penetrate the sample through the weakest point of the barrier. Inside the superconducting specimen, the vortices moving in bundles get randomly pinned at respective pinning sites such that the inter-vortex spacing is non-unique which leads to a non-uniform distribution of the flux-density. As mentioned earlier, the vortices are well separated at lower fields and therefore, the (elastic) interactions between them remain weak resulting in a stronger pinned (disordered) vortex configuration in the ZFC mode. Although the vortex

matter created in the FC mode also remains disordered at lower fields, however, the vortices in this mode nucleate more uniformly as they remain oblivious to disordering effects of the surface barriers and the non-uniform injection through edges, etc. Therefore, at lower fields, the vortex configuration in FC mode is less disordered than in the case of ZFC. At higher fields, as the vortices get closer to each other and hence, the interaction effects become dominant yielding a better spatial ordering even during the moving state of creation of vortex matter in the ZFC mode. On the other hand, during the FC mode, the vortex matter has to cross the PE boundary in the H - T phase space which results in supercooling the disordered vortex matter prevailing at the peak position of the PE anomaly. Thus, at higher fields, the vortex matter created in the ZFC mode is more spatially ordered than that in the FC mode.

V. CONCLUSION

We have investigated via magnetization measurements, a weakly - pinned single crystal of a low T_c superconductor, $\text{Yb}_3\text{Rh}_4\text{Sn}_{13}$. The present results have led to the identification of BG to VG transition line and sketch of a characteristic field ($H^*(T)$) line in the H - T phase space of this compound. Surprisingly, the SMP transition like phase boundary has been unearthed under the combined influence of an ac driving force and a continuous magnetic field sweeping involved in the (isothermal) ac susceptibility ($\chi'(H)$) measurements. This transition was, however, not observed in the (isothermal) dc M - H loops and the temperature-dependent ac susceptibility scans ($\chi'(T)$). The latter two modes of measurements yield signature of only the quintessential PE anomaly signaling the collapse of elasticity of vortex solid at higher fields. An apparent demarcation between the domain of SMP like transition and the onset of PE anomaly has been made in the vortex phase diagram of $\text{Yb}_3\text{Rh}_4\text{Sn}_{13}$. The results presented in our specimen answer in affirmative the question of generic nature of BG to VG transition in a pinned superconductor. These also find supports from another experimental study [45] at microscopic level in a sample of the same compound. In the low field region ($H < H^*$), the vortex matter is construed to be highly disordered. Here, a vortex state created in the FC mode is found to be more ordered than that obtained in the ZFC mode.

Acknowledgments

Santosh Kumar would like to acknowledge the Council of Scientific and Industrial Research, India for the grant of the Senior Research Fellowship. Santosh Kumar wishes to thank Ulhas Vaidya for his help and assistance in the use of SVSM system in TIFR, Mumbai in the initial phase of work.

-
- [1] T. Giamarchi and P. Le. Doussal, Phys. Rev. Lett. 72, 1530 (1994).
- [2] T. Giamarchi and P. Le. Doussal, Phys. Rev. B 52, 1242 (1995).
- [3] S. S. Banerjee, A. K. Grover, M. J. Higgins, Gutam I. Menon, P. K. Mishra, D. Pal, S. Ramakrishnan, T. V. Chandrasekhar Rao, G. Ravikumar, V. C. Sahni, S. Sarkar, C. V. Tomy, Physica C 355, 39 (2001) and references therein.
- [4] T. Giamarchi and P. Le. Doussal, Phys. Rev. B 55, 6577 (1997).
- [5] M. Daeumling, J. M. Seuntjens and D. C. Larbalestier, Nature (London) 346, 332 (1990).
- [6] B. Khaykovich, E. Zeldov, D. Majer, T. W. Li, P. H. Kes and M. Konczykowski, Phys. Rev. Lett. 76, 2555 (1996).
- [7] B. Khaykovich, M. Konczykowski, E. Zeldov, R. A. Doyle, D. Majer, P. H. Kes and T. W. Li, Phys. Rev. B 56, R517 (1997).
- [8] T. Nishizaki, N. Kobayashi, Supercond. Sci. Technol. 13, 1 (2001).
- [9] D. Pal, S. Ramakrishnan, A. K. Grover, D. Dasgupta, B. K. Sarma, Phys. Rev. B 63, 132505 (2001).
- [10] S. Sarkar, D. Pal, P. L. Paulose, S. Ramakrishnan, A. K. Grover, C. V. Tomy, D. Dasgupta, Bimal, K. Sarma, G. Balakrishnan, D. McK Paul, Phys. Rev. B 64, 144510 (2001).
- [11] D. Giller, B. Kalisky, I. Shapiro, B. Ya. Shapiro, A. Shaulov, Y. Yeshurun, Physica C 388, 731 (2003).
- [12] A. B. Pippard, Philos. Mag. 19, 217 (1969).
- [13] M. J. Higgins, S. Bhattacharya, Physica C 257, 232 (1996) and references therein.
- [14] H. Sato, Y. Aoki, H. Sugawara, T. Fukuhara, J. Phys. Soc. Jpn. 64, 3175 (1995).
- [15] C. V. Tomy, G. Balakrishnan, D. McK. Paul, Physica C 280, 1 (1997).
- [16] S. Sarkar, S. Banerjee, A. K. Grover, S. Ramakrishnan, S. Bhattacharya, G. Ravikumar, P. K. Mishra, V. C. Sahni, C. V. Tomy, D. McK. Paul, G. Balakrishnan, M. J. Higgins, Physica C 341, 1055 (2000).
- [17] X. S. Ling, S. R. Park, B. A. McClain, S. M. Choi, D. C. Dender, J. W. Lynn, Phys. Rev. Lett. 86, 712 (2001).
- [18] Santosh Kumar, Ravi P. Singh, A. Thamizhavel, C. V. Tomy and A. K. Grover, Physica C 506, 69 (2014).
- [19] W. Henderson, E. Y. Andrei, M. J. Higgins and S. Bhattacharya, Phys. Rev. Lett. 77, 2077 (1996).
- [20] S. S. Banerjee, N. G. Patil, S. Ramakrishnan, A. K. Grover, S. Bhattacharya, G. Ravikumar, P. K. Mishra, T. V. Chandrasekhar Rao, V. C. Sahni and M. J. Higgins, Appl. Phys. Lett. 74, 126 (1999).
- [21] S. S. Banerjee, N. G. Patil, S. Ramakrishnan, A. K. Grover, S. Bhattacharya, P. K. Mishra, G. Ravikumar, T. V. Chandrasekhar Rao, V. C. Sahni, M. J. Higgins, C. V. Tomy, G. Balakrishnan and D. McK Paul, Phys. Rev. B 59, 6043 (1999).
- [22] G. Ravikumar, V. C. Sahni, P. K. Mishra, T. V. Chandrasekhar Rao, S. S. Banerjee, A. K. Grover, S. Ramakrishnan, S. Bhattacharya, M. J. Higgins, E. Yamamoto, Y. Haga, M. Hedo and Y. Inada, Y. Onuki, Phys. Rev. B 57, R11069 (1998).
- [23] G. P. Espinosa, Mater. Res. Bull. 15, 791 (1980).
- [24] C.P. Bean, Rev. Mod. Phys. 36, 31 (1964).
- [25] W.A. Fietz and W.W. Webb, Phys. Rev. 178, 657 (1969).
- [26] M. Marchevsky, M. J. Higgins and S. Bhattacharya, Nature 409, 591 (2001).
- [27] X. S. Ling and J. Budnick in Magnetic Susceptibility of Superconductors and Other Spin Systems, edited by R. A. Hein, T. L. Francavilla, D. H. Liebenberg (Plenum Press, New York, 1991), p. 377.
- [28] Y. Paltiel, E. Zeldov, Y. Myasoedov, M. L. Rappaport, G. Jung, S. Bhattacharya, M. J. Higgins, Z. L. Xiao, E. Y. Andrei, P. L. Gammel and D. J. Bishop, Phys. Rev. Lett. 85, 3712 (2000).
- [29] G. Ravikumar, H. Kupfer, A. Will, R. Meier-Hirmer and Th. Wolf, Phys. Rev. B 65, 094507, (2002).
- [30] A.I. Larkin and Yu. N. Ovchinnikov, Sov. Phys. JETP 38, 854 (1974).
- [31] A.I. Larkin and Yu. N. Ovchinnikov, J. Low Temp. Phys. 34, 409 (1979).
- [32] John R. Clem and Zhidong Hao, Phys. Rev. B 48, 13774 (1993).
- [33] S. O. Valenzuela and V. Bekeris, Phys. Rev. Lett. 84, 4200 (2000).
- [34] G. Ravikumar, K. V. Bhagwat, V. C. Sahni, A. K. Grover, S. Ramakrishnan and S. Bhattacharya, Phys. Rev. B 61, R6479 (2000).
- [35] G. Ravikumar, V. C. Sahni, A. K. Grover, S. Ramakrishnan, P. L. Gammel, D. J. Bishop, E. Bucher, M. J. Higgins and S. Bhattacharya, Phys. Rev. B 63, 024505 (2001).
- [36] G. Ravikumar and H Kupfer, Phys. Rev. B 72, 144530 (2005).
- [37] N. Avraham, B. Khaykovich, Y. Myasoedov, M. Rappaport, H. Shtrikman, D. E. Feldman, T. Tamegai, P. H. Kes, M. Li, M. Konczykowski, K. van der Beek, E. Zeldov, Nature 411, 451 (2001).
- [38] S. S. Banerjee *et al.*, Physica C 308, 25-32 (1998).
- [39] D. S. Fisher, M. P. A. Fisher, and D. A. Huse, Phys. Rev. B 43, 130 (1991)..
- [40] K. Ghosh, S. Ramakrishnan, A. K. Grover, Gautam I. Menon, Girish Chandra, T. V. Chandrasekhar Rao, G. Ravikumar, P. K. Mishra, V. C. Sahni, C. V. Tomy, G. Balakrishnan, D. McK Paul, S. Bhattacharya, Phys. Rev. Lett. 76, 4600 (1996).
- [41] M. J. P. Gingras and D. A. Huse, Phys. Rev. B 53, 15193 (1996).
- [42] D. Pal, D. Dasgupta, Bimal K Sarma, S. Bhattacharya, S. Ramakrishnan and A. K. Grover, Phys. Rev. B 62, 6699 (2000).
- [43] D.G. Grier, C.A. Murray, C.A. Bolle, P.L. Gammel, D.J. Bishop, D.B. Mitzi, and A. Kapitulnik, Phys. Rev. Lett. 66, 2270 (1992).
- [44] S. Horiuchi, M. Cantoni, M. Uchida, T. Tsuruta, and Y. Matsui, Appl. Phys. Lett. 73, 1293 (1998).
- [45] D. Mazzone, J. L. Gavilano, R. Sibille, M. Ramakrishnan, C. D. Dewhurst, and M. Kenzelmann, arXiv:1407.0569v2 [cond-mat.supr-con] 22 Oct 2014.
- [46] Y. Paltiel, D. T. Fuchs, E. Zeldov, Y. N. Myasoedov, and H. Shtrikman, M. L. Rappaport and E. Y. Andrei, Phys. Rev. B 58, R14763 (1998).
- [47] Y. Paltiel, E. Zeldov, Y. N. Myasoedov, H. Shtrikman, S. Bhattacharya, M. J. Higgins, Z. L. Xiao, E. Y. Andrei, P. L. Gammel and D. J. Bishop, Nature (London) 403,

398 (2000).